Journal of Materials Chemistry A

PAPER

Cite this: J. Mater. Chem. A, 2016, 4, 10493

High-performance free-standing PEDOT:PSS electrodes for flexible and transparent all-solid-state supercapacitors†

Tao Cheng,[a] Yi-Zhou Zhang,[a] Jian-Dong Zhang,[a] Wen-Yong Lai*[ab] and Wei Huang[ab]

Received 28th April 2016
Accepted 9th June 2016

DOI: 10.1039/c6ta03537j

www.rsc.org/MaterialsA

High-performance free-standing PEDOT:PSS electrodes with not only superior optoelectronic performance and high flexibility but also excellent electrochemical performance were successfully fabricated *via* facile multilayer spin-coating of a doped PEDOT:PSS solution. Superior optoelectronic performance and high electrochemical performance could be simultaneously achieved *via* doping PEDOT:PSS and modulating the layer numbers of the spin-coated PEDOT:PSS. Flexible and transparent all-solid-state supercapacitors with both superior electrochemical performance and relatively high optical transparency were fabricated for the first time using the resultant high-performance PEDOT:PSS films as both the current collectors and the active electrodes.

Introduction

Flexible and transparent energy conversion and storage devices, such as organic solar cells and thin-film supercapacitors, are currently acknowledged as promising technologies that will become building blocks of future integrated power sources.[1–11] The unique mechanical flexibility and the optical transparency greatly expand the application scope ranging from flexible displays to automobile windshields, smart building windows, non-planar translucent tops, and modern recreational facilities, such as portable and wearable electronics.[12,13] To meet the demands of emerging flexible and transparent energy conversion and storage devices, the most fundamental component of electronic devices, the electrode, should not only possess superior optoelectronic performance and high flexibility but also excellent electrochemical performance.

Indium tin oxide (ITO) is presently the most widely used transparent electrode due to its excellent optoelectronic performance, but its fragile nature and high cost as well as complicated manufacturing method constrain its further applications in future flexible devices. Recently, a novel class of electrode materials, including metal nanowires,[14–20] metal grids,[21–24] carbon nanotubes (CNTs),[25,26] graphene[1,27] and conductive polymers,[28–33] have been intensively explored to substitute ITO. Metal nanowires and metal grids with high flexibility and superior optoelectronic performance have been used as transparent electrodes for optoelectronic devices as previously reported.[20,24] However, metal based transparent electrodes are somewhat unsuitable for energy storage devices due to their lack of capacitive behaviours. Carbon nanomaterials, such as graphene and carbon nanotubes, generally have superb flexibility and electric double-layer capacitance (EDLC) behaviours, showing wide applications in flexible supercapacitors.[1,34,35] Nevertheless, their optoelectronic performance is usually limited by their low conductivity; thus a thick film is needed to enhance the conductivity, which inevitably reduces the optical transmittance, unsuitable for optoelectronic devices. Conductive polymers, especially poly(3,4-ethylene dioxythiophene):(styrene sulfonate) (PEDOT:PSS), possess multifarious potential advantages, including high optical transmittance, tunable conductivity and electrochemical performance as well as excellent flexibility.[28,29,31,36,37] Thus, they show great potential for applications as multifunctional flexible transparent electrodes that are not only viable for optoelectronic devices such as solar cells but also suitable for energy storage devices such as supercapacitors.

Various hybrid electrodes composed of PEDOT:PSS and carbon nanomaterials or metal oxides have recently been explored for supercapacitors with superior electrochemical performance.[26,38–41] However, the relatively low optoelectronic performance limited by the low optical transmittance of the hybrid electrodes constrains their application in transparent supercapacitors and solar cells. Recently, free-standing single PEDOT:PSS based electrodes with high conductivity and superior electrochemical performance have been simultaneously used in high performance solid-state supercapacitors and solar cells but the very thick PEDOT:PSS film also led to low optical

[a]Key Laboratory for Organic Electronics & Information Displays (KLOEID) & Institute of Advanced Materials (IAM), Jiangsu National Synergetic Innovation Center for Advanced Materials (SICAM), Nanjing University of Posts & Telecommunications, 9 Wenyuan Road, Nanjing 210023, China. E-mail: iamwylai@njupt.edu.cn

[b]Key Laboratory of Flexible Electronics (KLOFE) & Institute of Advanced Materials (IAM), Jiangsu National Synergetic Innovation Center for Advanced Materials (SICAM), Nanjing Tech University, 30 South Puzhu Road, Nanjing 211816, China

† Electronic supplementary information (ESI) available: Effect of doping on the conductivity, morphology and electrochemical performance of the PEDOT:PSS films. Optical transmittance of the device. See DOI: 10.1039/c6ta03537j

transmittance that is adverse to obtaining transparent energy devices.[28] Although the electrochemical performance of a transparent PEDOT:PSS electrode was systematically investigated in liquid electrolytes,[32] the application of transparent PEDOT:PSS electrodes in all-solid-state supercapacitors with both high optical transmittance and flexibility has never been reported to the best of our knowledge. Thus, the development of a multifunctional electrode that simultaneously exhibits superior optoelectronic performance and high electrochemical performance as well as the study of its application in flexible and transparent all-solid-state supercapacitors are vital to integrated power sources for buildings and especially future portable and wearable electronics.

In this work, high-performance free-standing PEDOT:PSS electrodes with not only superior optoelectronic performance, high flexibility and smooth morphology but also excellent electrochemical performance were successfully fabricated *via* facile multilayer spin-coating of a doped PEDOT:PSS solution. Superior optoelectronic performance and high electrochemical performance could be simultaneously achieved *via* doping the PEDOT:PSS and modulating the layer numbers of the spin coated PEDOT:PSS. The influence of the doping surfactant on the performance of the PEDOT:PSS electrodes, including morphology, optoelectronic performance and the electrochemical performance, was systematically investigated. It was found that 2 vol% surfactant can not only enhance the electrical conductivity but also improve the electrochemical performance of the PEDOT:PSS electrodes. Additionally, 2 vol% surfactant also improved the wettability and reduced the surface tension of the PEDOT:PSS layers, which was favourable for the subsequent coating and especially the multilayer spin coating of the PEDOT:PSS films to form a uniform and smooth surface morphology. Flexible and transparent all-solid-state supercapacitors with both superior electrochemical performance and relatively high optical transparency using the resultant high-performance PEDOT:PSS films as both the current collectors and the active electrodes were fabricated for the first time.

Experimental

Preparation of the PEDOT:PSS electrodes

The original PEDOT:PSS solution (PH1000) was filtered with 0.22 μm syringe filters followed by mixing with 6 vol% EG and 2 vol% surfactant. The resultant solution was sonicated to obtain a uniformly mixed formulation. PEDOT:PSS electrodes with one layer were fabricated *via* spin coating the resulting formulation on PET substrates at 500 rpm for 6 s followed by coating at 1500 rpm for 50 s. The electrodes were then annealed at 120 °C for 15 min after spin coating. PEDOT:PSS electrodes with multilayers were prepared using almost the same conditions as those for the PEDOT:PSS electrodes with one layer except that the electrodes need to be annealed before coating the next layer.

Preparation of the all-solid-state supercapacitors

The electrolyte was prepared by mixing PVA powder (1.0 g), H_3PO_4 (1.0 g) and deionized water (10.0 mL). The mixture was then heated at 90 °C under stirring until it turned into a gel. The gel electrolyte was then coated on the PEDOT:PSS/PET followed by drying in air at room temperature. Finally, two such electrolyte coated PEDOT:PSS electrodes were assembled into a supercapacitor by pressing them together.

Results and discussion

Fig. S1a and b† illustrate the sheet resistance of single-layer PEDOT:PSS with an optical transmittance of ~94% changing with the volume of the dopants. As shown in Fig. S1a,† the sheet resistance of the pristine PEDOT:PSS layer was as large as around 0.4 MΩ sq.$^{-1}$. Intriguingly, the sheet resistance gradually decreased with the increment of the amount of ethylene glycol (EG) and it dramatically decreased to ~140 Ω sq.$^{-1}$ when 6 vol% EG was added. However, the sheet resistance remained nearly constant when the volume of the added EG was more than 6%. ~6 vol% EG proved to be the optimal concentration to improve the conductivity.[29,31] To further enhance the electrical conductivity, a different volume of the surfactant (Triton-X 100) was then added to the PEDOT:PSS solution doped with 6 vol% EG. The sheet resistance of the 6 vol% EG doped PEDOT:PSS was further reduced when the volume of the doped surfactant was increased from 0% to 2%. When the volume of the added surfactant was more than 2%, the sheet resistance showed a slight increase instead compared with the 2 vol% doped PEDOT:PSS, as illustrated in Fig. S1b.† The sheet resistance was reduced to ~110 Ω sq.$^{-1}$ when 2 vol% surfactant was added.

The surfactant not only reduced the sheet resistance but also improved the wettability and decreased the surface tension of PEDOT:PSS, which was favourable for the subsequent spin-coating and especially the multilayer spin-coating of PEDOT:PSS. As shown in Fig. S2a,† a non-uniform morphology was clearly observed in the 6 vol% EG doped PEDOT:PSS multilayer. By contrast, a uniform and smooth PEDOT:PSS film morphology was observed when 2 vol% surfactant was added, as illustrated in Fig. S2b.† Fig. 1a is the photograph of a flexible and transparent PEDOT:PSS electrode with four layers. Fig. 1b is the scanning electron microscopy (SEM) image of the surface morphology of the electrode, from which a uniform and well-connected film can be clearly identified. Fig. 1c and d are the corresponding two dimensional (2D) and three dimensional (3D) atomic force microscopy (AFM) images. The average surface roughness (R_a) and the root-mean-square (rms) surface roughness of the PEDOT:PSS electrodes (four layers) were ~1.2 nm and ~1.5 nm, respectively, suggesting that the resultant electrodes exhibited a smooth morphology. The uniform and smooth morphology obtained in the spin-coated PEDOT:PSS multilayers mainly originated from the improved wettability and the reduced surface tension caused by the doped surfactant.

Fig. 2a and b illustrate the optoelectronic performance of PEDOT:PSS with various layer numbers. It was observed that the optical transmittance and the sheet resistance were simultaneously reduced with the increase of layer numbers. The sheet resistance of the PEDOT:PSS films with one to five layers was ~145 Ω sq.$^{-1}$, ~65 Ω sq.$^{-1}$, ~48 Ω sq.$^{-1}$, ~36 Ω sq.$^{-1}$ and ~27

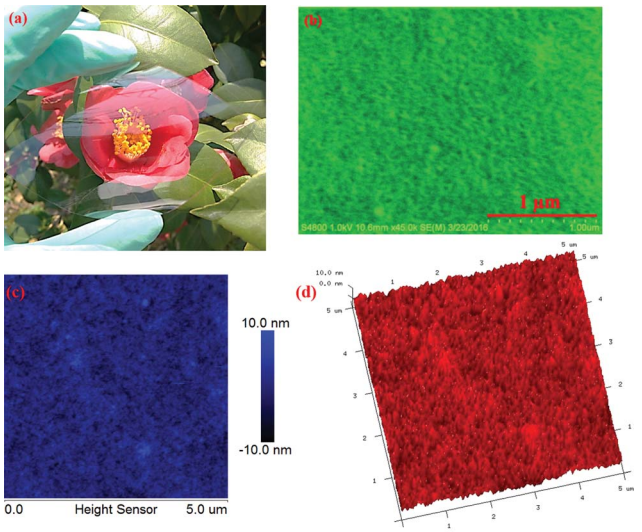

Fig. 1 (a) Photograph of the resultant PEDOT:PSS electrode (four layers). (b) The SEM image of the surface morphology. (c) The 2D and (d) 3D AFM images of the PEDOT:PSS electrode with four layers.

Ω sq.$^{-1}$ while their optical transmittance was ~95%, ~89%, ~87%, ~82% and ~78%, respectively. The superior optoelectronic performance of the resultant PEDOT:PSS electrodes was even comparable to that of some best-performing metal based transparent electrodes, such as Cu nanowires,[42] Cu@Cu_4Ni nanowires[43] and Ag grids.[24]

Besides superior optoelectronic performance, the resultant PEDOT:PSS electrodes also exhibited comparatively high flexibility. Fig. 2c and d show their sheet resistance under bending tests. As illustrated by the insets of Fig. 2c, the PEDOT:PSS/PET electrodes were clamped by two block clips which can be freely moved forward and backward. The PEDOT:PSS/PET electrode could be bent to various degrees *via* moving the clip that clamped one end of the PEDOT:PSS/PET electrode towards the other clip. The D/L of the horizontal axis in Fig. 2c is the ratio of the displacement (D) of the clip accounting for the original length (L) of the electrode. It is apparent that the larger the D/L, the stronger the bending. The bending degrees of the electrodes were 0°, ~60°, ~90° and ~180° when the value of D/L was 0%, 12.5%, 25% and 50%, respectively. The electrodes were nearly folded (~180°) in half when D/L increased to 50%. As shown in Fig. 2c, the sheet resistance of the PEDOT:PSS electrodes with

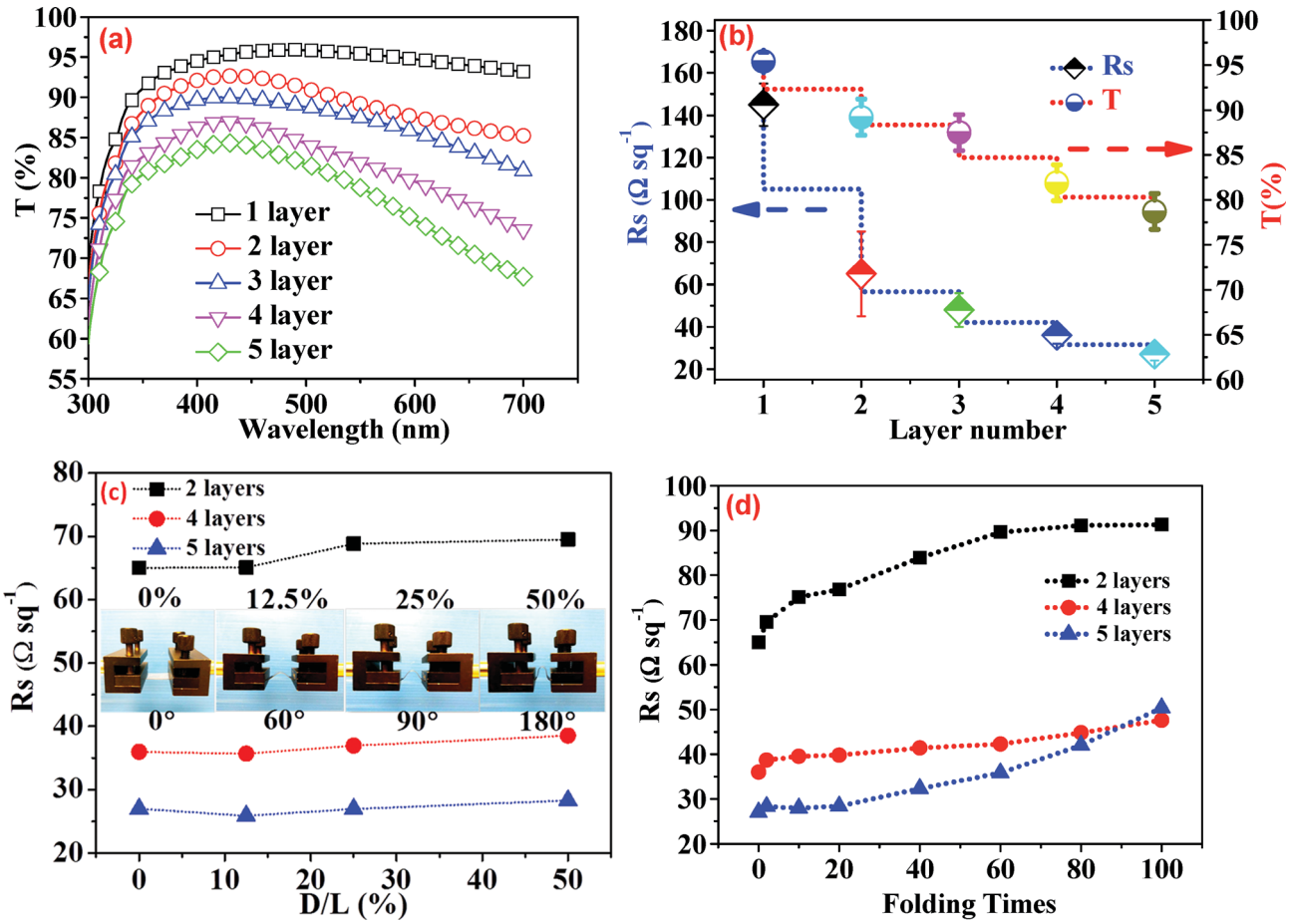

Fig. 2 (a) The optical transmittance *versus* the wavelength of the PEDOT:PSS electrodes with different spin-coating layer numbers. (b) The sheet resistance and the optical transmittance of the PEDOT:PSS electrodes changing with the layer number. (c) The sheet resistance of the PEDOT:PSS electrodes under various bending states. (d) The sheet resistance changing with the folding times.

two, four and five layers only increased slightly with the increment of the D/L. Moreover, keeping D/L constant at 50%, the electrodes were repeatedly folded one hundred times, and the sheet resistance of the three electrodes with different layers just increased by much less than one time compared with the original value, demonstrating their superior flexibility.

Fig. 3 shows the optical microscopy images of the morphology of the PEDOT:PSS electrodes with various layer numbers before and after being bent. Fig. 3a–c show the original morphology of the PEDOT:PSS electrodes with two, four and five layers, respectively, in which smooth films were observed. The other images with different magnifications illustrate the morphology of the three PEDOT:PSS electrodes after being folded one hundred times. It could be seen that wrinkle-like structures formed in the films after being folded, which partly decreased the electrical conductivity of the PEDOT:PSS electrodes.

The electrochemical performance of the PEDOT:PSS electrodes was investigated in flexible and transparent all-solid-state supercapacitors with a symmetrical sandwiched structure, as shown in Fig. 4a. The PEDOT:PSS electrodes were used as both the current collectors and the active electrodes. It deserves to be mentioned that the amount of the doped surfactant not only influenced the electrical conductivity of the PEDOT:PSS electrodes but also affected their electrochemical performance. Fig. S3a† shows the cyclic voltammetry (CV) curves (100 mV s^{-1}) of the supercapacitors based on PEDOT:PSS (one layer) electrodes doped with different volumes of the surfactant. Obviously, the capacitive behaviours gradually improved with the increment of the surfactant volume. The 2 vol% surfactant doped PEDOT:PSS showed the best capacitive behaviours with the most saturated CV curve. Fig. S2b† shows the corresponding galvanostatic charge–discharge (GCD) curves and it could be observed that the supercapacitor based on 2 vol% surfactant doped PEDOT:PSS electrodes also exhibited the longest discharging time. When the volume of the doped surfactant surpassed 2%, the capacitive behaviours got worse instead. Strikingly, the tendency of the electrochemical performance changing with the amount of the surfactant accorded comparatively well with that of the electrical conductivity. The ~2 vol% surfactant was the optimum value for improving both the electrical conductivity and the electrochemical performance of the PEDOT:PSS electrodes. The capacitive behaviours were improved when the volume of the surfactant was increased from 0 to 2 vol% because the sheet resistance reduced with the increment of the surfactant, which was beneficial to the transportation and the collection of the ions. When the doped surfactant was more than 2 vol%, the PEDOT:PSS got too viscous and some defects formed in the PEDOT:PSS film; thus the supercapacitors showed slightly worse electrical conductivity and electrochemical stability during the electrochemical test. Fluctuation of the CV and GCD curves was commonly observed, leading to relatively bad capacitive behaviours, as illustrated in Fig S3a and b.† Besides the amount of the surfactant, the influence of the film thickness on the electrochemical performance of the PEDOT:PSS electrodes was also systematically investigated while keeping the volume of the doped surfactant at 2%. Fig. 4b shows the CV curves of the supercapacitors based on the PEDOT:PSS electrodes with different layers at a constant scan rate of 100 mV s^{-1}. Notably, the current density of the supercapacitors gradually increased with the increment of the PEDOT:PSS layers. The discharging time also prolonged with the increase of the PEDOT:PSS layers, as illustrated by the GCD curves (Fig. 4c) at a constant current density of 0.025 mA cm^{-2}. Fig. 4d and e are the CV and GCD curves of the supercapacitors based on the PEDOT:PSS electrodes with four layers. Both the nearly rectangular shape of the CV curves even at a high scan rate of 500 mV s^{-1} and the typical

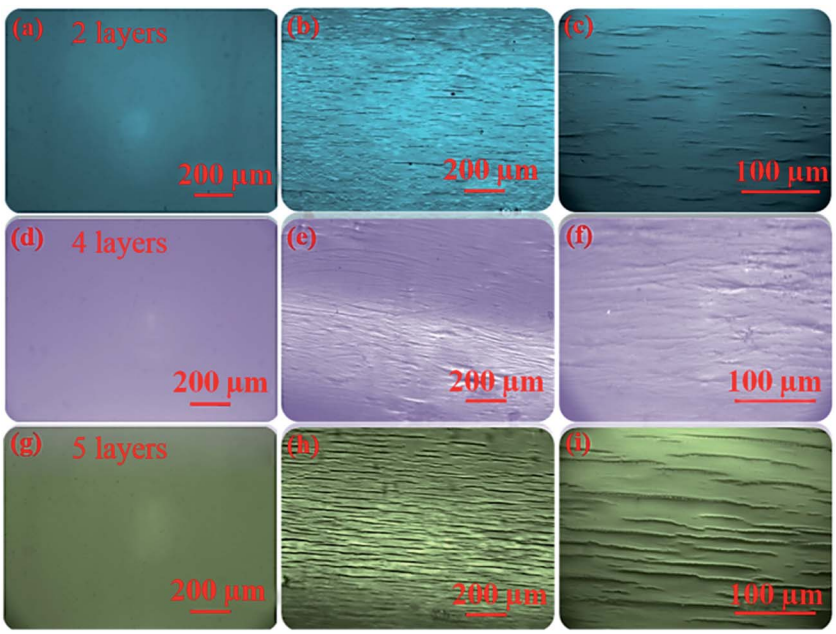

Fig. 3 The optical microscopy images of the morphology of the PEDOT:PSS electrodes with two, four and five layers before and after being bent.

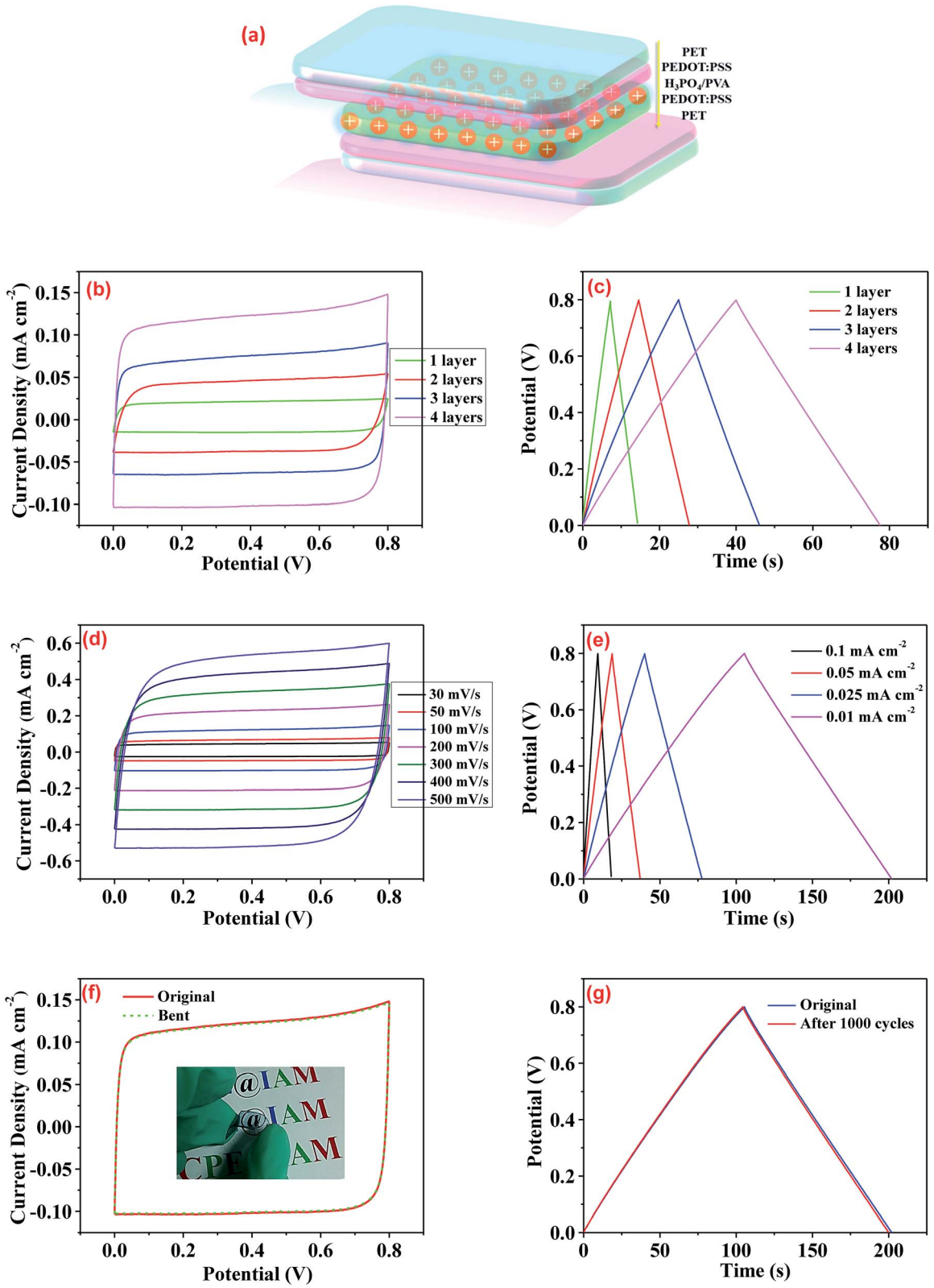

Fig. 4 (a) Structure of the all-solid-state supercapacitor. (b) CV curves of the supercapacitors based on the PEDOT:PSS electrodes with different layers at a constant scan rate of 100 mV s^{-1}. (c) GCD curves of the supercapacitors based on the PEDOT:PSS electrodes with different layers at a current density of 0.025 mA cm^{-2}. (d) CV curves of the supercapacitors based on the PEDOT:PSS electrodes with four layers at various scan rates. (e) GCD curves of the supercapacitors based on the PEDOT:PSS electrodes with four layers at various current densities. (f) CV curves of the supercapacitors based on the PEDOT:PSS electrodes with four layers without bending and under bending at a scan rate of 100 mV s^{-1} and the inset is the photograph of the flexible and translucent all-solid-state supercapacitor under the bending state. (g) Cyclic stability test of the supercapacitors.

triangular shape of the GCD curves demonstrated that the supercapacitors possessed excellent capacitive behaviours. The areal specific capacitance (C), energy density (E) and the power density (P) can be calculated using the following equations:

$$C_t = \frac{I\Delta t}{S\Delta V} \quad (1)$$

$$C_{sc} = 4C_t \quad (2)$$

$$E = \frac{1}{2}C_t\Delta V^2 \quad (3)$$

$$P = \frac{E}{\Delta t} \quad (4)$$

where C_t is the specific capacitance of the supercapacitor, C_{sc} is the specific capacitance of the electrode, I is the discharge current, Δt is the discharging time, S is the effective area and ΔV is the voltage window. The mass loading of the supercapacitors with different PEDOT:PSS layers was 0.038 mg cm^{-2}, 0.057 mg cm^{-2}, 0.12 mg cm^{-2} and 0.17 cm^2, respectively. The areal specific capacitance and the gravimetric specific capacitance of the supercapacitors based on the PEDOT:PSS electrodes with one, two, three and four layers were 0.23 mF cm^{-2} (6.05 F g^{-1}), 0.41 mF cm^{-2} (7.19 F g^{-1}), 0.66 mF cm^{-2} (5.50 F g^{-1}), and 1.18 mF cm^{-2} (6.94 F g^{-1}), respectively. The corresponding areal/gravimetric specific capacitance of the electrode was 0.92 mF cm^{-2} (24.20 F g^{-1}), 1.64 mF cm^{-2} (28.76 F g^{-1}), 2.64 mF cm^{-2} (22.0 F g^{-1}), and 4.72 mF cm^{-2} (27.76 F g^{-1}) calculated from Fig. 4c. The areal specific capacitance was improved with the increase of the PEDOT:PSS layers, suggesting larger electrochemical storage capability of the supercapacitors with more PEDOT:PSS layers. This was mainly because the mass of the active materials, namely the PEDOT, also increased with the layers. The energy density was 0.074 mW h cm^{-2}, 0.13 mW h cm^{-2}, 0.21 mW h cm^{-2} and 0.38 mW h cm^{-2} while the power density was nearly constant at ~0.036 W cm^{-2} regardless of the increase of the PEDOT:PSS layer number. Both the areal specific capacitance and the energy density were enhanced when the PEDOT:PSS layer number was increased from one to four. It is anticipated that the areal specific capacitance and the energy density can be further improved using PEDOT:PSS electrodes with more than four layers. However, the optical transparency of the supercapacitors was reduced with the increment of the PEDOT:PSS layers, which was because the thicker the PEDOT:PSS layer, the stronger the absorbance. To realize an ideal balance between the electrochemical performance and the optical transparency of the supercapacitors, 3–4 layers of PEDOT:PSS are probably the most ideal electrodes for supercapacitors that simultaneously show superior electrochemical performance and high optical transparency. For example, the high C_t and the C_{sc} of the supercapacitors based on the PEDOT:PSS electrodes with four layers were 1.18 mF cm^{-2} and 4.72 mF cm^{-2}, which are comparable and even superior to those of some excellent supercapacitors previously reported.[4,32,35,44] Moreover, the areal specific capacitance remained nearly constant after 1000 charge–discharge cycles at a current density of 0.01 mA cm^{-2}, demonstrating relatively high cyclic stability, as illustrated in Fig. 4g. Apart from the superior electrochemical performance, the supercapacitors also exhibited comparatively high optical transparency. Fig. S4† shows the plot of the optical transmittance *versus* the wavelength of the supercapacitor. It could be seen that the optical transmittance was as high as 55–67% in the wavelength range from 400 nm to 600 nm. As shown by the inset in Fig. 4f, the words beneath the supercapacitor could be clearly seen, verifying the relatively high optical transparency. Additionally, the CV curves (at a scan rate of 100 mV s^{-1}) remained almost unchanged when the supercapacitor was highly bent, demonstrating its superior flexibility, as illustrated by Fig. 4f.

Conclusions

Free-standing PEDOT:PSS electrodes with superior optoelectronic performance, excellent electrochemical performance, high flexibility and smooth morphology were successfully fabricated *via* facile multilayer spin coating of a doped PEDOT:PSS solution. Superior optoelectronic performance and high electrochemical performance were simultaneously realized *via* doping the PEDOT:PSS and modulating the number of the PEDOT:PSS layers. The simultaneous realization of superior optoelectronic performance and high electrochemical performance in the PEDOT:PSS electrodes is vital to the development of flexible and transparent energy conversion and storage devices as well as to the future integrated power sources for modern human society. As a demonstration, flexible all-solid-state supercapacitors with both superior electrochemical performance and relatively high optical transparency using the resultant high-performance PEDOT:PSS films as current collectors and active electrodes were fabricated for the first time.

Acknowledgements

We acknowledge financial support of the National Key Basic Research Program of China (973 Program, 2014CB648300), the National Natural Science Foundation of China (21422402, 20904024, 51173081, 61136003), the Natural Science Foundation of Jiangsu Province (BK20140060, BK20130037, BM2012010), the Program for Jiangsu Specially-Appointed Professors (RK030STP15001), the Program for New Century Excellent Talents in University (NCET-13-0872), Specialized Research Fund for the Doctoral Program of Higher Education (20133223110008 and 20113223110005), the Synergetic Innovation Center for Organic Electronics and Information Displays, the Priority Academic Program Development of Jiangsu Higher Education Institutions (PAPD), the NUPT "1311 Project", the Six Talent Plan (2012XCL035), the 333 Project (BRA2015374) and the Qing Lan Project of Jiangsu Province.

Notes and references

1 B. Y. Xia, Y. Yan, X. Wang and X. W. Lou, *Mater. Horiz.*, 2014, **1**, 379.

2 T. Cheng, Y. Zhang, W. Y. Lai and W. Huang, *Adv. Mater.*, 2015, **27**, 3349.
3 J. Huang, G. Li and Y. Yang, *Adv. Mater.*, 2008, **20**, 415.
4 T. Chen, Y. Xue, A. K. Roy and L. Dai, *ACS Nano*, 2014, **8**, 1039.
5 T. Chen, H. Peng, M. Durstock and L. Dai, *Sci. Rep.*, 2014, **4**, 3612.
6 T. Ameri, G. Dennler, C. Waldauf, H. Azimi, A. Seemann, K. Forberich, J. Hauch, M. Scharber, K. Hingerl and C. J. Brabec, *Adv. Funct. Mater.*, 2010, **20**, 1592.
7 H. Y. Jung, M. B. Karimi, M. G. Hahm, P. M. Ajayan and Y. J. Jung, *Sci. Rep.*, 2012, **2**, 773.
8 Z. Niu, W. Zhou, J. Chen, G. Feng, H. Li, Y. Hu, W. Ma, H. Dong, J. Li and S. Xie, *Small*, 2013, **9**, 518.
9 Y. Z. Zhang, Y. Wang, T. Cheng, W. Y. Lai, H. Pang and W. Huang, *Chem. Soc. Rev.*, 2015, **44**, 5181.
10 Y. Z. Zhang, Y. Wang, Y. L. Xie, T. Cheng, W. Y. Lai, H. Pang and W. Huang, *Nanoscale*, 2014, **6**, 14354.
11 B.-U. Hwang, J.-H. Lee, T. Q. Trung, E. Roh, D.-I. Kim, S.-W. Kim and N.-E. Lee, *ACS Nano*, 2015, **9**, 8801.
12 W. Liu, C. Lu, H. Li, R. Y. Tay, L. Sun, X. Wang, W. L. Chow, X. Wang, B. K. Tay, Z. Chen, J. Yan, K. Feng, G. Lui, R. Tjandra, L. Rasenthiram, G. Chiu and A. Yu, *J. Mater. Chem. A*, 2016, **4**, 3754.
13 G. Cai, P. Darmawan, M. Cui, J. Wang, J. Chen, S. Magdassi and P. S. Lee, *Adv. Energy Mater.*, 2016, **6**, 1501882.
14 J. Lee, P. Lee, H. B. Lee, S. Hong, I. Lee, J. Yeo, S. S. Lee, T.-S. Kim, D. Lee and S. H. Ko, *Adv. Funct. Mater.*, 2013, **23**, 4171.
15 J. Liang, L. Li, X. Niu, Z. Yu and Q. Pei, *Nat. Photonics*, 2013, **7**, 817.
16 D. Shin, T. Kim, B. T. Ahn and S. M. Han, *ACS Appl. Mater. Interfaces*, 2015, **7**, 13557.
17 Z. Zhu, T. Mankowski, K. Balakrishnan, A. S. Shikoh, F. Touati, M. A. Benammar, M. Mansuripur and C. M. Falco, *ACS Appl. Mater. Interfaces*, 2015, **7**, 16223.
18 A. R. Rathmell and B. J. Wiley, *Adv. Mater.*, 2011, **23**, 4798.
19 S. Ye, A. R. Rathmell, I. E. Stewart, Y.-C. Ha, A. R. Wilson, Z. Chen and B. J. Wiley, *Chem. Commun.*, 2014, **50**, 2562.
20 T. Cheng, Y.-Z. Zhang, W.-Y. Lai, Y. Chen, W.-J. Zeng and W. Huang, *J. Mater. Chem. C*, 2014, **2**, 10369.
21 G. Cai, P. Darmawan, M. Cui, J. Wang, J. Chen, S. Magdassi and P. S. Lee, *Adv. Energy Mater.*, 2016, **6**, 1501882.
22 H. Wu, D. Kong, Z. Ruan, P.-C. Hsu, S. Wang, Z. Yu, T. J. Carney, L. Hu, S. Fan and Y. Cui, *Nat. Nanotechnol.*, 2013, **8**, 421.
23 Y. H. Kim, L. Mueller-Meskamp and K. Leo, *Adv. Energy Mater.*, 2015, **5**, 1401822.
24 S. Hong, J. Yeo, G. Kim, D. Kim, H. Lee, J. Kwon, H. Lee, P. Lee and S. H. Ko, *ACS Nano*, 2013, **7**, 5024.
25 X. Wang, L. Zhi and K. Mullen, *Nano Lett.*, 2008, **8**, 323.
26 G. Yu, X. Xie, L. Pan, Z. Bao and Y. Cui, *Nano Energy*, 2013, **2**, 213.
27 S. Bae, H. Kim, Y. Lee, X. Xu, J. S. Park, Y. Zheng, J. Balakrishnan, T. Lei, H. R. Kim, Y. I. Song, Y. J. Kim, K. S. Kim, B. Ozyilmaz, J. H. Ahn, B. H. Hong and S. Iijima, *Nat. Nanotechnol.*, 2010, **5**, 574.
28 Z. Li, G. Ma, R. Ge, F. Qin, X. Dong, W. Meng, T. Liu, J. Tong, F. Jiang, Y. Zhou, K. Li, X. Min, K. Huo and Y. Zhou, *Angew. Chem., Int. Ed.*, 2016, **55**, 979.
29 J. P. Thomas and K. T. Leung, *Adv. Funct. Mater.*, 2014, **24**, 4978.
30 N. Kim, S. Kee, S. H. Lee, B. H. Lee, Y. H. Kahng, Y. R. Jo, B. J. Kim and K. Lee, *Adv. Mater.*, 2014, **26**, 2268.
31 Y. H. Kim, C. Sachse, M. L. Machala, C. May, L. Müller-Meskamp and K. Leo, *Adv. Funct. Mater.*, 2011, **21**, 1076.
32 T. M. Higgins and J. N. Coleman, *ACS Appl. Mater. Interfaces*, 2015, **7**, 16495.
33 X. Fan, J. Wang, H. Wang, X. Liu and H. Wang, *ACS Appl. Mater. Interfaces*, 2015, **7**, 16287.
34 P. Simon and Y. GoGotsi, *Nat. Mater.*, 2008, **7**, 845.
35 Z.-S. Wu, Z. Liu, K. Parvez, X. Feng and K. Müllen, *Adv. Mater.*, 2015, **27**, 3669.
36 T. Tevi, S. W. S. Birch, S. W. Thomas and A. Takshi, *Synth. Met.*, 2014, **191**, 59.
37 S. H. Lee, J. S. Sohn, S. B. Kulkarni, U. M. Patil, S. C. Jun and J. H. Kim, *Org. Electron.*, 2014, **15**, 3423.
38 S. Cho, M. Kim and J. Jang, *ACS Appl. Mater. Interfaces*, 2015, **7**, 10213.
39 Y. Liu, B. Weng, J. M. Razal, Q. Xu, C. Zhao, Y. Hou, S. Seyedin, R. Jalili, G. G. Wallace and J. Chen, *Sci. Rep.*, 2015, **5**, 17045.
40 C. Yin, C. Yang, M. Jiang, C. Deng, L. Yang, J. Li and D. Qian, *ACS Appl. Mater. Interfaces*, 2016, **8**, 2741.
41 Y. Hou, Y. Cheng, T. Hobson and J. Liu, *Nano Lett.*, 2010, **10**, 2727.
42 S. Han, S. Hong, J. Ham, J. Yeo, J. Lee, B. Kang, P. Lee, J. Kwon, S. S. Lee, M. Y. Yang and S. H. Ko, *Adv. Mater.*, 2014, **26**, 5808.
43 J. Song, J. Li, J. Xu and H. Zeng, *Nano Lett.*, 2014, **14**, 6298.
44 J. Ren, L. Li, C. Chen, X. Chen, Z. Cai, L. Qiu, Y. Wang, X. Zhu and H. Peng, *Adv. Mater.*, 2013, **25**, 1155.